# Macrophages are required to coordinate mouse digit tip regeneration

Jennifer Simkin[1,4] (jennifer.simkin@uky.edu)*, Mimi C. Sammarco[1,5] (msammarc@tulane.edu)*, Luis Marrero[3] (lmarre@lsuhsc.edu), Lindsay A. Dawson[1,2] ldawson@cvm.tamu.edu), Mingquan Yan[1,2] (myan@cvm.tamu.edu), Catherine Tucker[1] (ctucker3@tulane.edu), Alex Cammack[1] (acammack@tulane.edu), Ken Muneoka[1,2] (kmuneoka@cvm.tamu.edu)§

[1]Division of Developmental Biology, Department of Cell and Molecular Biology, Tulane University, New Orleans, LA 70118, USA
[2]Department of Veterinary Physiology and Pathology, College of Veterinary Medicine, Texas A&M University, College Station, TX 77843
[3]Morphology and Imaging Core Laboratory, Louisiana Health Sciences Center, New Orleans, 70112

[4]Current Address: Department of Biology, University of Kentucky, Lexington, KY 40508

[5]Current Address: Department of Surgery, Tulane School of Medicine, New Orleans 70112

*Equal contribution to work
§Author of correspondence:

Ken Muneoka
Department of Veterinary Physiology and Pathology,
College of Veterinary Medicine,
Texas A&M University, College Station, TX 77843

FAX 979 845-6544
Email: **kmuneoka@cvm.tamu.edu**

No conflict of interest to declare

**ABSTRACT**

In mammals, macrophages are known to play a major role in tissue regeneration. These cells contribute to inflammation, histolysis, re-epithelialization, re-vascularization and cell proliferation. While macrophages have been shown to be essential for regeneration in salamanders and fish, their role has not been elucidated in mammalian epimorphic regeneration. Here, using the regenerating mouse digit tip as a mammalian model, we demonstrate that macrophages are essential for the regeneration process. Using cell depletion strategies, we show that regeneration is completely inhibited; bone histolysis does not occur, wound re-epithelization is inhibited and the blastema does not form. While rescue of epidermal wound closure, in the absence of macrophages, promotes blastema accumulation it does not rescue cell differentiation indicating that macrophages play a key role in the re-differentiation of the blastema. Further, we provide additional evidence that while bone degradation is a part of the regenerative process, it is not essential to the overall regenerative process. These findings show that macrophages play an essential role in coordinating the epimorphic regenerative response in mammals.

Keywords: Regeneration, Mammal, Epimorphic, Blastema, Macrophage, Osteoclasts

## INTRODUCTION

While all animals display some level of regenerative ability, some just do it better. Among vertebrates, urodele amphibians possess the ability to faithfully regenerate large parts of their body, for example their limbs (Brockes, 1997), while a number of fish species including zebrafish, readily regenerate their tail fins (Gemberling et al., 2013; Pfefferli and Jazwinska, 2015). These examples involve the coordinated regeneration of multiple tissues. This process is mediated by the formation of a blastema, a heterogeneous population of cells that can re-enter the cell cycle and re-utilize developmental mechanisms to replace lost structures (Brockes and Kumar, 2002; Bryant et al., 2002; Stocum and Cameron, 2011; Tanaka, 2003). Blastema-mediated regeneration, called epimorphic, is considered to be distinct from the regeneration of individual damaged tissues, such as skin and bone, which undergo a repair response without forming a blastema (Carlson, 2005). In general, mammals display tissue-specific regenerative abilities (i.e. healing bone fractures) but a limited capacity to coordinate a multi-tissue regenerative response.

Among mammals there are only a few models of epimorphic regeneration, and the developing and adult digit tip of the mouse is the best characterized (Borgens, 1982; Fernando et al., 2011; Han et al., 2008; Neufeld and Zhao, 1993). Digit tip regeneration in mice parallels the regeneration of human fingertips, a process well documented in the clinical literature (Illingworth, 1974; McKim, 1932), and displays characteristics that are similar to amphibian models of limb regeneration including blastema formation (Fernando et al., 2011; Han et al., 2008). Amputation of an adult mouse terminal phalangeal element (P3) transects the nail plate, epidermis, dermis which includes loose connective tissue, blood vessels and nerves, bone, and bone marrow (Simkin et al., 2013). Thus the primary structural tissues that regenerate are bone, including bone marrow, and skin, including epidermis and its derivatives as well as the heterogeneous dermis. When studied as separate tissues, skin and bone undergo very different healing responses than that observed during the coordinated multi-tissue digit regeneration response.

The repair of mammalian skin has been studied primarily in full thickness wounds in which the healing response consists of distinct but overlapping phases beginning with hemostasis/inflammation, the formation of granulation tissue and finally, matrix remodeling (Eming et al., 2014). The inflammatory response dominates the early stages of healing and is critical for re-epithelization as well as supporting granulation tissue formation (DiPietro et al., 1998; Goren et al., 2009; Leibovich and Ross, 1975; Mirza et al., 2009). Later, during matrix remodeling, the immature scar tissue deposited by granulation tissue is realigned and cross-linked to form the mature scar (Xue and Jackson, 2015). The wound healing process involves a balance between inflammatory and anti-inflammatory signals but overall, is not considered regenerative (i.e. dermal patterning is not restored and epidermal structures do not regrow), and depletion of macrophages, neutrophils and inflammatory signals results in less granulation tissue formation and a scar-free regenerative healing response (Ashcroft et al., 1999; Martin et al., 2003; Mori et al., 2002). Thus, high numbers of macrophages appear to function in an inhibitory way. Alternatively, tissue-specific bone regeneration has been studied in the context of fracture healing and consists of distinct overlapping phases that begins with inflammation and ends with remodeling of the regenerated bone (Schindeler et al., 2008). Macrophage depletion studies show that these cells are required for bone regeneration and successful fracture healing (Alexander et al., 2011; Raggatt et al., 2014). Thus, in a bone regeneration model, macrophages play an essential and stimulatory role in the regeneration of new bone.

It is not intuitively obvious how the epimorphic regenerative properties of the digit tip relate to the tissue specific repair properties of bone (regenerative) and skin (non-regenerative). Nevertheless, both repair responses initiate with inflammation; in the case of wound healing, its action is largely inhibitory whereas in fracture healing its action is stimulatory. Inflammation in mammalian epimorphic regeneration has not been investigated although recent studies in urodele limb and zebrafish fin regeneration show that macrophages are required for regeneration (Godwin et al., 2013; Petrie et al., 2014). We use the mouse digit tip to investigate the effects of macrophages during a mammalian epimorphic regeneration response. In this study, we focus on cells of the monocytic

lineage including macrophages and osteoclasts. Monocytic cell depletion inhibits bone degradation, wound re-epithelization, blastema formation and completely inhibits the regenerative response. Conversely, enhancing macrophage numbers does not have a major effect on the regeneration response. Coupling monocyte cell depletion with the rescue of wound re-epithelization rescues blastema formation but does not rescue regeneration. On the other hand, targeted depletion of osteoclasts coupled with rescuing wound re-epithelization inhibits bone degradation but does not inhibit blastema formation and regeneration. Thus if wound re-epithelization is stimulated, regeneration occurs in the absence of active osteoclasts but not in the absence of active macrophages. With these data we conclude that wound re-epithelization is a macrophage-dependent process that is required for blastema accumulation. Finally these results suggest macrophages play a prominent role in the re-differentiation stage of regeneration, independent of a role in osteoclastogenesis or wound re-epithelization.

## RESULTS

### Both neutrophils and macrophages accumulate at the injury site after digit amputation.

To characterize the inflammation response following mouse digit amputation, immunohistochemical techniques were used to analyze the timing and position of $CD45^+$ hematopoietic cells, $Ly6B.2^+$ neutrophils (Hirsch and Gordon, 1983) and $F4/80^+$ macrophages (Austyn and Gordon, 1981) within the amputation wound (Fig. 1A). Wound closure following digit tip amputation is a lengthy process taking 8-9 days and involves circumferential healing of the epidermis onto dead stump bone (Fernando et al., 2011; Simkin et al., 2015a). The cells of the amputation wound response are therefore localized to the periphery of the amputated P3 bone. Prior to and immediately following amputation, there are few neutrophils or macrophages present in the mature digit (Fig. 1B,F). Indeed, there are few CD45 positive cells in the mature digit indicating that the pool of resident cells of the hematopoietic cell lineage prior to amputation injury is very low (Fig. 1J). Following amputation we find a progressive influx of neutrophils within digit stump tissues that

peaks at 5 days post amputation (DPA) (ANOVA main effect time, F= 10.54 p=0.0002; *Bonferroni post hoc test $p<0.05$). Ly6B.2$^{+}$ cells associated with the scab at 3 DPA appear to be dead or dying, while neutrophils present in the stump are mainly present in the bone marrow cavity (Fig. 1C arrows). At 7 DPA the wound epidermis is not yet closed; neutrophils are localized to the bone marrow and the dermal connective tissue surrounding the bone stump (Fig 1D). When the blastema forms by 10 DPA, neutrophils are predominately localized to the blastema and the bone marrow cavity (Fig 1E). By 15 DPA, neutrophil numbers return to pre-amputation levels (Fig. 1A).

Following digit amputation, macrophage numbers peak at 7 DPA and return to baseline by 21 DPA (Fig. 1A, ANOVA with main effect time, F=3.18, p=0.04, *Bonferroni post hoc test $p<0.05$). The spatial localization of F4/80$^{+}$ cells at selected timepoints was somewhat variable across animals and this is reflected in Figure 1. We did however, notice a few trends. F4/80+ cells are seen in low numbers in the bone marrow immediately following amputation (Fig 1F). At 3 DPA, macrophages are scattered within the bone marrow and also in the connective tissue surrounding the P3 stump (Fig 1G). At 7 and 10 DPA, macrophages are found in high numbers within the dermis associated with the nail matrix, and by 10 DPA, F4/80$^{+}$ cells also line the endosteal layer of the P3 bone marrow (Fig. 1H,I). Notably, once the blastema forms, few F4/80$^{+}$ macrophages are observed in the blastema itself (Fig. 1I) and this was consistent across all regenerates analyzed. Immunohistochemical staining of the pan-hematopoietic marker CD45 at similar regeneration stages identifies cells within the bone marrow, stump dermis, and blastema that overlap the combined staining for neutrophils and macrophages (Fig. 1K-M) and suggests that these cell types represent the majority of the hematopoietic response to digit amputation. Overall, the regeneration response is associated with an accumulation of neutrophils found predominately within the bone marrow and blastema, while macrophages are localized initially to the stump dermis associated with the nail matrix, and later to the endosteum of the P3 bone stump.

**Macrophages are required for digit tip regeneration.**

To explore the role that the macrophage population has in digit tip regeneration, we first tested the hypothesis that increasing macrophage presence inhibited regenerative capacity. We used targeted application of Macrophage Chemoattractant Protein (MCP-1/CCL2) following digit tip amputation to enhance the recruitment of activated macrophages (Dipietro et al., 2001). A micro-carrier bead soaked in a high concentration of MCP-1 (0.5µg/µl) was implanted in the connective tissue of the P3 digit. In uninjured digits this MCP-1 treatment is able to enhance macrophage recruitment over control BSA treated beads at 5 days post implantation (DPI), and macrophage levels returned to control levels by 15 days (Fig. 2A, *Bonferroni post hoc test, main effect treatment, $p<0.05$). When MCP-1 treatment was coupled with digit amputation, we observe a higher influx of macrophage numbers when compared to BSA-treated digits at 5 and 15 DPA (Fig. 2A, *Bonferroni post hoc test, main effect treatment $p<0.05$). The enhanced macrophage presence was observed in both the dermis and bone marrow (Fig. 2B,C). These data show that MCP-1 treatment successfully enhances and sustains macrophage recruitment to the regenerating amputation wound. Following the regeneration process using µCT in vivo imaging, we found that MCP-1 treated digits successfully regenerated largely in parallel with controls (Fig. 2D,E). Bone volume measurements during the regenerative response indicated a statistically significant reduction in bone degradation associated with MCP-1 treatment (Fig 2D *Bonferroni post hoc, main effect treatment $p<0.05$). This result was not anticipated based on evidence that MCP-1 enhances osteoclast differentiation in vitro and also enhances foreign body giant cell fusion in vivo (Khan et al., 2016; Kyriakides et al., 2004). Nevertheless, the findings indicate that enhancing F4/80$^{+}$ macrophage recruitment to the amputated digit does influence monocyte lineage cells but does not inhibit the regenerative response. These data do not support the hypothesis that macrophages are inhibitory for regeneration in mammals.

To explore the effect of depleting macrophage numbers during digit tip regeneration we used a commercially available reagent, Clodronate Liposomes, that is effective in transiently depleting macrophages when applied either systemically or locally (Alexander et al., 2011; Barrera et al., 2000;

Li et al., 2013; Xiang et al., 2012). Clodronate Liposomes are selectively engulfed by phagocytic cells and are cell lethal; however unengulfed liposomes are rapidly cleared (within 15 minutes) via the kidneys (van Rooijen and Hendrikx, 2010). We used a local Clodronate Liposome treatment of individual mouse digits during the rise in macrophage recruitment to test whether phagocytic cells are required for digit tip regeneration. Clodronate Liposomes (Clo-Lipo) or control liposomes containing PBS (PBS-Lipo) were injected into amputated digits at 0, 2 and 5 DPA. Samples were collected at 6 DPA to check for neutrophil and macrophage presence based on immunohistochemistry and for osteoclast presence based on distinct cytological characteristics, i.e. multinucleated giant cells with ruffled borders. We observed a significant reduction in F4/80$^{+}$ cells in Clo-Lipo injected digits as compared to PBS-Lipo controls indicating that targeted treatment effectively diminished, but did not eliminate, the local macrophage population (Fig. 3A, *unpaired student's t-test $p<0.05$). Osteoclasts which are derived from the monocyte/macrophage lineage (Sprangers et al., 2016) and are known to be present in high numbers during regeneration, (Fernando et al., 2011; Sammarco et al., 2014), were also depleted; a finding consistent with Clo-Lipo use in fracture healing (Alexander et al., 2011; Winkler et al., 2010). Neutrophils and osteoblasts are largely unaffected by Clo-Lipo treatment (Suppl. Fig. 1). These findings show that Clo-Lipo treatment is effective in locally depleting the injury-induced macrophage population.

To evaluate the effect of macrophage and osteoclast depletion on digit regeneration, we tracked anatomical and volumetric changes of the amputated P3 bone with µCT in Clo-Lipo and PBS-Lipo treated digits (Fig. 3B). 3D renderings of µCT scans show no change in bone architecture or bone volume over a 35 day period following amputation and Clo-Lipo treatment (Fig. 3B,C). Control digits exhibited a regeneration response similar to previous studies that included an initial bone volume decline prior to blastema formation followed by an average regrowth of 150% of the amputated stump bone volume (Fernando et al., 2011; Sammarco et al., 2015; Sammarco et al., 2014; Simkin et al., 2015b), thus indicating that the liposome vehicle did not alter the regenerative response (Fig. 3B,C). The data show that Clo-Lipo treatment inhibits both the bone degradation response and also the

regeneration of distal bone. We also carried out studies to explore both the dose and timing of Clo-Lipo treatment on the regeneration response. A single injection of Clo-Lipo at the time of amputation resulted in digits that either failed to regenerate (37.5%; 3/8) or regenerated abnormally (62.5%; 5/8) producing boney spikes from regions of the stump (Suppl. Fig. 2A). Bone architecture suggests that the degradation phase is completely inhibited by a single treatment with Clo-Lipo, and that bone redifferentiation by the blastema is not an all or none event. To explore the relationship between the Clo-Lipo effect and the timing of the inflammation response, a single treatment with Clo-Lipo was administered at the peak of the inflammation response (7 DPA). Treatment at this time shows a trend toward reduced bone degradation and re-differentiation responses, but treated samples were not statistically different from PBS-Lipo treated controls (Suppl. Fig. 3, Two-way ANOVA main effect time, $F=25.72$, $p<0.0001$, and main effect treatment $F=0.002$, $p=0.97$). These studies identify the early stages of the inflammation response as being critical for the regeneration promoting effect that phagocytic and histolytic cells, such as macrophages and osteoclasts, have on blastema formation and digit tip regeneration in mice.

**Epidermal closure and histolysis is suspended by Clo-Lipo treatment.**

To understand better Clo-Lipo inhibited regeneration we carried out a histological analysis on samples that were treated with Clo-Lipo or PBS-Lipo and focused on key stages of the normal regenerative response (Fig. 4). PBS-Lipo treated digits demonstrate a regenerative response similar to untreated digits characterized in previous publications (Fernando et al., 2011; Sammarco et al., 2015; Sammarco et al., 2014; Simkin et al., 2015b). Briefly, at 7 DPA control digits show an open amputation wound, extensive stump bone degradation associated with osteoclast filled bone pits, a hypercellular bone marrow and activated osteoblast lining the endosteum and periosteum (Fig. 4A). At 10 DPA control digits have a closed wound epidermis, a prominent blastema and histological evidence of new osteoid deposition in the interface between the proximal blastema and the stump (Fig. 4B). At DPA 13 new bone growth in the form of woven bone islands are prominent at the

blastema/stump interface (Fig. 4C arrowheads). At 28 DPA the regeneration of control digits is largely complete with the replacement of the digit tip that consist of newly regenerated woven bone, a reestablished distal marrow cavity, regenerated dermis and a regenerated distal nail plate (Fig. 4D).

In sharp contrast, the histology of Clo-Lipo treated digits show that the digit stump is largely unchanged during this 28 day period, and that the injury is suspended at an early phase of regeneration (Fig. 4E-H). There are a number of remarkable observations. First, there is no evidence of osteoclasts or bone pitting of the stump at any of the time points analyzed, and this is consistent with bone volume measurements from μCT imaging (Fig. 2B). Thus, Clo-Lipo treatment completely inhibits osteoclastogenesis and bone degradation typically associated with the regenerative response. Second, the epidermis fails to close over the amputation wound even by 28 DPA (Fig. 4H white arrows) indicating that Clo-Lipo treatment inhibits wound closure. However, the nail continues to elongate and creates a large distal pocket devoid of cells subjacent to the elongating nail (Fig. 4F, arrow). Thus, epidermal expansion and nail elongation does not appear to be dependent on either macrophages or the histolytic event. Third, we observe polymorphonuclear neutrophils associated with the amputation wound site (Fig. 4G inset) at all stages analyzed, suggesting that inflammation characteristics of the amputation wound is maintained and not completely resolved. Fourth, there is no histological evidence of blastema formation and no digit regeneration. Combined, these data suggest that disruption of the regenerative phase using Clo-Lipo depletion of macrophages and osteoclasts inhibits regeneration.

**The specific loss of osteoclasts delays bone degradation and results in impaired regeneration.**

Osteoclasts are multinucleated cells of the monocyte lineage so their absence in Clo-Lipo studies was anticipated, however, this combined depletion makes it difficult to differentiate between the effects of depleted macrophages and the effects of depleted osteoclasts. To further elucidate the influence of macrophages on digit regeneration we treated digits with free clodronate (F-Clo) which directly targets osteoclasts for depletion without affecting macrophages (Russell and Rogers, 1999).

To establish the efficacy of F-Clo, we administered a single injection of F-Clo into the digit at the time of amputation and evaluated osteoclast and macrophage presence at 7 DPA. Immunohistochemical studies show a distinct reduction of Cathepsin K positive osteoclasts when compared to PBS injected control digits (Fig. 5A,B). In contrast, F4/80 positive macrophages were abundant at the distal stump of P3 in F-Clo treated and PBS treated control digits (Fig. 5C,D). These data show that F-Clo treatment is effective in selectively depleting osteoclasts without impairing the macrophage population during digit tip regeneration, and this result is consistent with previous reports (Frith et al., 1997; Zeisberger et al., 2006). To study the effect of F-Clo on digit regeneration we measured changes in bone volume using μCT imaging following a single treatment with F-Clo at the time of amputation. Control digits injected with PBS undergo a normal regeneration response as previously described (see Fig. 2C,D). In contrast, digits receiving a single injection with F-Clo displayed an impaired regeneration response characterized by a delay in the onset of bone degradation and a reduced osteogenic response (Fig 5E,F; *Bonferroni post hoc test $p<0.05$, main effect treatment). Histological analysis at 11 DPA and 14 DPA showed that wound closure, blastema formation and regeneration are delayed in F-Clo treated digits (Fig. 5G).

To address the hypothesis that regeneration was dependent on osteoclasts and bone degradation, we took advantage of our previous finding that the degradation/re-epithelialization link can be uncoupled by stimulating rapid wound closure over the amputated stump with the cyanoacrylic wound dressing, Dermabond (Simkin et al., 2015b). To determine if osteoclasts are necessary for blastema formation and regeneration downstream of wound closure, we treated osteoclast-depleted and control digits with Dermabond. Based on histological analyses applying Dermabond to F-Clo- or PBS-treated digits stimulated epidermal closure by 7 DPA, and in both cases a blastema forms distal to the stump bone (Fig. 5H,I) that results in a regenerated digit (Fig. 5J,K). MicroCT imaging of F-Clo/ Dermabond and PBS/ Dermabond treated digits showed that the amount of bone degradation was reduced in PBS digits and completely inhibited in F-Clo digits (Fig. 5J). Nevertheless, both PBS control and F-Clo treated digits regenerated the amputated digit tip,

suggesting that the absence of osteoclasts is not inhibitory for regeneration if re-epithelialization is allowed to occur.

**Stimulating epidermal closure does not rescue Clo-lipo inhibition of regeneration.**

Because rescue of re-epithelialization promotes a regenerative response in osteoclast-depleted digits, we next tested if re-epithelization could rescue regeneration in a macrophage-depleted (Clo-Lipo injected) digit. We first established that Dermabond rescues the wound closure deficit that results from macrophage depletion and that re-epithelization is complete by 7 DPA (Fig. 6A,B). Clo-Lipo/ Dermabond treated digits do not show evidence of bone degradation but develop a distal accumulation of cells (Fig. 6B). This aggregate of cells is not observed at a later time point (DPA 28, Fig. 6D). We used μCT imaging to track anatomical and bone volume changes of the digits during the regenerative response. In control studies combining Dermabond wound dressing with PBS-Lipo treatment we observed a regenerative response similar to that observed following only Dermabond treatment, whereas digits treated with Dermabond and Clo-Lipo displayed no change in stump bone volume or anatomy (Fig. 6C, D) indicating the absence of a regeneration response. These studies show that rescuing wound closure is not sufficient to rescue the regeneration response caused by combined osteoclast/macrophage depletion. The data show that the wound epidermis is able to recruit cells to form a blastema-like accumulation of cells, however this population of cells fails to progress to differentiated bone, indicating that the final stages of blastema differentiation is macrophage dependent. Overall, these studies indicate that osteoclasts and macrophages play a role in the early regeneration stages (i.e. re-epithelialization and bone degradation), but that macrophages specifically are required for final stages of digit regeneration (i.e. maintenance and differentiation of the blastema).

## DISCUSSION

In adult mammals, the resolution of traumatic injury throughout the body is tissue specific: some tissues undergo impaired healing with little sign of regeneration (e.g. skin, heart) whereas other tissues are able to regenerate a functional replacement (e.g. bone, skeletal muscle, liver) (Stocum, 2012). In all of these tissues the injury response involves inflammation that includes the mobilization and invasion of macrophages. A key goal in regeneration biology is preventing pathological outcomes from uncontrolled infection or fibrosis and enhancing restoration of tissue function. Macrophages are essential in protecting the host from infection and, more recently, have been shown to be essential in promoting regenerative responses (Godwin et al., 2013; Petrie et al., 2014). Our current study expands upon these experiments in salamanders and fish, providing evidence that macrophages are essential for epimorphic regeneration in mammals as well. Thus these cells, as protectors from infection and promoters of repair, provide interesting targets for the field of regenerative medicine.

To use these cells as therapeutic interventions for regenerative medicine, the prominent question is one of timing; at what stage are macrophages necessary for an epimorphic regeneration response? In the current study, we used the regenerating digit tip of the mouse to show that macrophage invasion is essential for every stage of regeneration. Macrophage depletion causes an inhibition of osteoclastogenesis and bone degradation, re-epithelization, blastema formation, and redifferentiation of the blastema to reform the digit tip. Rescue of these individual stages narrows down specific roles for macrophages during regeneration. We find macrophages are required for osteoclastogenesis and bone degradation, but our data suggest this process itself is not required for a successful regenerative response. On the other hand, we find macrophages are essential for re-epithelization of the wound and the wound epidermis is required for blastema formation. Finally, macrophages are required for blastema cell differentiation in a manner independent of both degradation and re-epithelization. Overall, the evidence suggests that epimorphic regeneration in a mammalian model is macrophage-dependent and that macrophages regulate multiple key components of the regeneration response.

**Osteoclasts and bone degradation are not required for regeneration**

Osteoclasts are generally viewed as a bone-specific resident macrophage population, having the same progenitor cell as tissue macrophages (Sinder et al., 2015). Similar to previous studies of macrophage depletion in fracture healing (Alexander et al., 2011; Winkler et al., 2010), we find that Clo-Lipo injections effectively deplete both tissue macrophages and local osteoclasts subsequently inhibiting both bone degradation and regeneration. While it is clear that osteoclasts play a histolytic role in the regeneration response, it has not been clear whether the degradation of bone is required for a regenerative response. There is evidence implicating the bone degradation response in regulating blastema size and the extent of the regenerative response (Sammarco et al., 2015). Studies in other models of epimorphic regeneration show that histolytic activity is up-regulated early in regeneration and that matrix metalloproteinase activity plays a role in regenerate patterning (Bai et al., 2005; Grillo et al., 1968; Vinarsky et al., 2005; Yang and Bryant, 1994; Yang et al., 1999). In mouse digit regeneration we provide evidence that wound closure signals the termination of the bone degradation phase and transitions the regeneration response to blastema formation (Simkin et al., 2015b). Here we show that the use of clodronate to selectively deplete osteoclasts and delay degradation combined with enhancing wound closure to precociously terminate degradation completely eliminates bone degradation without depleting the macrophage population. The results show clearly that blastema formation and regeneration still occurs under conditions in which there is no anatomical evidence of bone degradation, thus it is clear that histolysis of the bone stump, although a prominent feature of the regeneration response, is not required for an epimorphic regenerative response in mice. In parallel, fracture healing studies show that osteoclast-specific depletion in a tissue-specific model of bone regeneration is not required for the osteogenic response (Alexander et al., 2011).

**The wound epidermis is required for blastema accumulation**

Local depletion of macrophages during digit tip regeneration leads to a complete inhibition of re-epithelization. Similar results from tissue-specific wound healing studies have been reported

(Leibovich and Ross, 1975; Lucas et al., 2010; Mirza et al., 2009) indicating that macrophages are required for re-epithelization in mammalian full thickness wounds. In digit amputation, we have previously shown that re-epithelization can be enhanced simply by treating the amputation wound with a cyanoacrylic wound dressing, Dermabond (Simkin et al., 2015b), and we show in the current study that Dermabond rescues re-epithelization inhibited by macrophage and osteoclast depletion. Such rescue is consistent with the conclusion that macrophages play a role in creating a wound environment permissive for re-epithelization rather than having a direct effect on epidermal cells. The lack of an apparent effect on epidermal expansion and nail elongation in macrophage-depleted digits also supports this conclusion.

Because macrophage depletion inhibits the formation of the wound epidermis, blastema formation and blastema differentiation we are able to explore the relationship between these events. Dermabond stimulates the formation of a wound epidermis and rescues regeneration in osteoclast-depleted digits but does not rescue regeneration in macrophage-depleted digits. In macrophage-depleted digits, the wound epidermis does stimulate the accumulation of a population of cells that appear blastema-like distal to the amputation stump. While the regenerative potential of this structure will require further examination, these data suggests the wound epidermis plays a major role in recruiting cells distal to the amputation injury. We find that without macrophages these cells do not differentiate into new tissues of the digit. The necessity of the wound epidermal and mesenchymal cell interactions for epimorphic regeneration is established in other models such as salamander limb regeneration and zebrafish fin regeneration (Carlson, 1969; Chablais and Jazwinska, 2010; Goss, 1956; Mescher, 1976; Whitehead et al., 2005) and in the mouse digit, WNT signaling derived from epidermal cells has been shown to be necessary for regeneration (Lehoczky and Tabin, 2015; Takeo et al., 2013). However our studies suggest that macrophages are a necessary intermediate in these epidermal-mesenchymal interactions for complete digit regeneration.

**Macrophages play multiple roles in epimorphic regeneration**

During traumatic injury the inflammatory response must navigate a fine balance between the initial protection against infection versus the eventual promotion of a functional repair response (Godwin et al., 2016). In classical epimorphic regeneration models, such as the salamander limb or the zebrafish fin, recent macrophage depletion studies provide clear evidence that this balance is tipped toward the promotion of a functional regeneration response (Godwin et al., 2013; Petrie et al., 2014), and our study adds the mouse digit tip to this list of macrophage-dependent regenerative responses. Epimorphic regeneration in adult mammals is relatively rare whereas the regeneration of specific tissues such as muscle and bone can be quite robust. Other tissues, such as the skin, display regenerative responses only during specific developmental stages (fetal) or in selective regions of the body (e.g. oral skin), whereas adult skin typically undergoes a non-regenerative healing response that culminates in the deposition of scar tissue (Mak et al., 2009; Martin and Leibovich, 2005). It is interesting that the inflammation response is known to promote the regeneration of bone and muscle tissue, while inhibiting regenerative healing full thickness skin wounds (Martin et al., 2003; Mori et al., 2008; Novak et al., 2014; Raggatt et al., 2014). These observations point to the evolution of an inflammatory balance between the initial protection against infection that drive the response in skin wounds versus the promotion of regenerative responses of internal tissues, e.g. muscle and bone, that is necessary for body function and survival. It is interesting that some of the macrophage activities identified in epimorphic regeneration parallel established tissue-specific responses of skin (e.g. promotion of re-epithelization) and bone (e.g. promotion of osteogenesis). Thus the data supports the idea that what makes epimorphic regeneration unique is the way in which multiple tissue-specific responses are coordinated both temporally and spatially, and that macrophages play a key role in this process. This conclusion also helps to bridge the interface between epimorphic and tissue-specific regenerative responses, and provides an avenue for the development of strategies to enhance regeneration in mammals.

## MATERIALS AND METHODS

### Digit amputations and animal care

Adult 8-week old female CD1 mice were obtained from Charles River Laboratories (Wilmington, MA). Mice were anesthetized with 1-5% isoflurane gas with continuous inhalation. The second and fourth digits of both hind limbs were amputated at the P3 distal level as described previously (Simkin et al., 2013). Digits were collected at specified time points for histological analysis. All experiments were performed in accordance with the standard operating procedures approved by the Institutional Animal Care and Use Committees at Tulane University Health Sciences Center and the College of Veterinary Medicine at Texas A&M University.

### Histology and Immunohistochemistry

Tissue was harvested at specified time points and fixed in Zinc buffered formalin (Anatech, Battle Creek, MI) overnight. Bone was decalcified for 8 hours in formic acid based decalcifier (Decal I, Surgipath, Richmond, IL). Samples were processed for paraffin embedding using a Leica TP 1020 Processor (Leica, Buffalo Grove, IL). 4 μm serial sections were obtained using a Leica RM2255 microtome. Sections were deparaffinized in xylenes and rehydrated through a series of graded ethanol. Mayer's Hematoxylin and Eosin Y (Sigma-Aldrich, St. Louis, MO) staining was carried out according to manufacturer's protocol. Mallory Trichrome staining was also carried out according to manufacturer's instructions (American Mastertech, Lodi, CA). Coverslips were mounted with Permount mounting medium (Fisher Scientific, Waltham, MA). For immunohistochemistry, serial sections were deparaffinized in xylene and rehydrated through graded ethanol. Antigen retrieval was carried out in either a pH6 citrate buffer for 20 minutes at 90°C or with proteinase K at 10mg/mL for 10 minutes at 37°C according to in-house optimized protocols for each antibody. Endogenous hydrogen peroxide was blocked using a solution of 3% $H_2O_2$ in methanol, and endogenous avidin and biotin were blocked with a Dako blocking kit. Non-specific antibody binding sites were blocked using a serum free blocking buffer (Dako, Carpinteria, CA). Slides were incubated at 4°C overnight

with the following primary antibodies: F4/80 (5µg/mL, Rat anti mouse, Cat# 14-4801, eBioscience, San Diego, CA), Ly6B.2 (0.1µg/mL, Rat anti mouse, Cat# MCA771A, AbD Serotec/BioRad), Cathepsin K (2µg/mL, Rabbit anti mouse, Cat# 19027, Abcam, Cambridge, MA), CD45 (5µg/mL, Rat anti mouse, Cat# 103101, BioLegend, San Diego, CA). Primary antibody detection was carried out using either secondary antibodies conjugated to Alexa Fluor 488 and 568 (Invitrogen, Carlsbad, CA) or secondary antibodies conjugated to biotin and resolved with a tyramide amplification kit according to manufacturer's instructions (TSA kit #T20912, Invitrogen / ThermoFisher Scientific).

**Image analysis**

Brightfield images of histological sections were obtained using a 10x, 20x or 40x objective on an Olympus BX60 upright microscope equipped with an Olympus DP72 camera. Fluorescent micrographs were acquired on an Olympus BX61 fluorescence deconvolution microscope. Quantification of fluorescent signal was performed using masking subsampling of positive fluorescent area in Slidebook Imaging Software (Intelligent Imagine Innovations, Denver, CO). Total area of 488 or 568nm fluorescent signal was calculated and normalized to total DAPI area to calculate % positive area / total cellular area. Signal quantification was restricted to the connective tissue area, excluding nail, epidermis, scab, bone and bone marrow. The entire P3 area of a representative section of each sample was imaged for quantification at 10x magnification. Autofluorescent red blood cells were subtracted from images using a Slidebook subtraction algorithm before quantification to reduce background signal.

**MCP-1 bead implants**

400µm Cibacron blue Affi-gel agarose beads (BioRad) are soaked in 0.5 mg/mL MCP1 (Prospec, Cat# CHM-313) with 0.1% BSA in PBS. Vehicle control beads were soaked in 0.1% BSA in PBS. Bead implants were carried out as previously described (Simkin et al., 2013). Briefly, after soaking in protein solution overnight, beads were allowed to air dry and were implanted with tungsten needles

into the dermis surrounding the P3 bone at 0 or 3 DPA. For each treated mouse, digits on one paw received PBS soaked beads and on the other paw MCP1 soaked beads. Left/right paw treatment was randomized for each mouse. Macrophage recruitment was calculated with immunofluorescent analysis as described above.

**Osteoclast, Macrophage depletion and rescue of re-epithelization**

For macrophage or osteoclast depletion, 10μL of 50mg/mL Clodronate liposomes (Clo-Lipo), or PBS liposomes (PBS-Lipo, www.ClodronateLiposomes.com) was injected into the P2 region of each amputated digit using an insulin syringe. Each digit received an injection at 0, 2, and 5 DPA. For depletion of osteoclasts, Clodronate (1.85μg/g body weight) was injected in 10μL of PBS into the P2 region just prior to digit amputation. For control digits, 10μL of PBS was injected alone. Depletion efficacy was quantified by immunofluorescence for Cathepsin K and F4/80+ cells. For rescue of wound closure experiments, 10μL of Dermabond (Ethicon, LLC, San Lorenzo, Puerto Rico) was applied to each digit immediately following amputation. Digits were allowed to dry for 1 minute following Dermabond application and then injected with Clo-Lipo, PBS-lipo, F-Clo or PBS.

**Micro-CT analysis**

Micro-CT images were acquired using a VivaCT 40 (Scanco Medical AG, Bruttisellen, Switzerland) at 1000 projections per 180 degrees with a voxel resolution of $10\mu m^3$, and energy and intensity settings of 55V and 145μA respectively. Integration time for capturing the projections was set to 380 ms using continuous rotation. Images were segmented using the BoneJ (Doube et al., 2010) (Version 1.2.1) Optimize Threshold Plugin for ImageJ (Version1.48c). Changes in bone volume were quantified using the BoneJ Volume Fraction Plugin for ImageJ. Percent bone volume divided by total bone volume (% BV/TV) was calculated by normalizing the measurement of each digit to its original volume immediately following amputation. Final images were compiled using Adobe Photoshop CS4 and CS6.

### Statistical analysis

Bone volume graphs were compiled and were analyzed using Two-way ANOVA with main effects treatment and time using JMP (v. 10.0.0, SAS Institute Inc.). Bonferroni multiple comparison tests were conducted for simple effect treatment at specific time points when appropriate and reported on the graphs. Graphs of immuno-positive area for cell counting studies were compiled and analyzed using Prism (version 6, Graphpad). Two-way ANOVA with main effects time and treatment or unpaired Student's t-test for simple effect treatment were calculated as indicated in figure legends. All figures were compiled using Adobe Photoshop and Adobe Illustrator (Creative Suite 6).

## ACKNOWLEDGEMENTS

The authors thank members of the Muneoka lab, Larry Suva and Dana Gaddy for discussions. Funding for this project was provided by W911NF-06-1-0161 from DARPA, W911NF-09-1-0305 from the US Army Research Center, the John L. and Mary Wright Ebaugh endowment fund at Tulane University, and Texas A&M University. The authors have no conflicts of interest to declare.

## REFERENCES


**Alexander, K. A., Chang, M. K., Maylin, E. R., Kohler, T., Muller, R., Wu, A. C., Van Rooijen, N., Sweet, M. J., Hume, D. A., Raggatt, L. J., et al.** (2011). Osteal macrophages promote in vivo intramembranous bone healing in a mouse tibial injury model. *J Bone Miner Res* **26**, 1517-1532.

**Ashcroft, G. S., Yang, X., Glick, A. B., Weinstein, M., Letterio, J. J., Mizel, D. E., Anzano, M., Greenwell-Wild, T., Wahl, S. M. and Deng, C.** (1999). Mice lacking Smad3 show accelerated wound healing and an impaired local inflammatory response. *Nature cell biology* **1**, 260-266.

**Austyn, J. M. and Gordon, S.** (1981). F4/80, a monoclonal antibody directed specifically against the mouse macrophage. *Eur J Immunol* **11**, 805-815.

**Bai, S., Thummel, R., Godwin, A. R., Nagase, H., Itoh, Y., Li, L., Evans, R., McDermott, J., Seiki, M. and Sarras, M. P., Jr.** (2005). Matrix metalloproteinase expression and function during fin regeneration in zebrafish: analysis of MT1-MMP, MMP2 and TIMP2. *Matrix biology : journal of the International Society for Matrix Biology* **24**, 247-260.

**Barrera, P., Blom, A., van Lent, P. L., van Bloois, L., Beijnen, J. H., van Rooijen, N., de Waal Malefijt, M. C., van de Putte, L. B., Storm, G. and van den Berg, W. B.** (2000). Synovial macrophage depletion with clodronate-containing liposomes in rheumatoid arthritis. *Arthritis Rheum* **43**, 1951-1959.

**Borgens, R. B.** (1982). Mice regrow the tips of their foretoes. *Science* **217**, 747-750.

**Brockes, J. P.** (1997). Amphibian limb regeneration: rebuilding a complex structure. *Science* **276**, 81-87.

**Brockes, J. P. and Kumar, A.** (2002). Plasticity and reprogramming of differentiated cells in amphibian regeneration. *Nat Rev Mol Cell Biol* **3**, 566-574.

**Bryant, S. V., Endo, T. and Gardiner, D. M.** (2002). Vertebrate limb regeneration and the origin of limb stem cells. *Int J Dev Biol* **46**, 887-896.

**Carlson, B. M.** (1969). Inhibition of limb regeneration in the axolotl after treatment of the skin with actinomycin D. *The Anatomical Record* **163**, 389-401.

**Carlson, B. M.** (2005). Some principles of regeneration in mammalian systems. *Anatomical record. Part B, New anatomist* **287**, 4-13.

**Chablais, F. and Jazwinska, A.** (2010). IGF signaling between blastema and wound epidermis is required for fin regeneration. *Development* **137**, 871-879.

**DiPietro, L. A., Burdick, M., Low, Q. E., Kunkel, S. L. and Strieter, R. M.** (1998). MIP-1alpha as a critical macrophage chemoattractant in murine wound repair. *Journal of Clinical Investigation* **101**, 1693.

**Dipietro, L. A., Reintjes, M. G., Low, Q. E., Levi, B. and Gamelli, R. L.** (2001). Modulation of macrophage recruitment into wounds by monocyte chemoattractant protein-1. *Wound Repair Regen* **9**, 28-33.

**Doube, M., Klosowski, M. M., Arganda-Carreras, I., Cordelieres, F. P., Dougherty, R. P., Jackson, J. S., Schmid, B., Hutchinson, J. R. and Shefelbine, S. J.** (2010). BoneJ: Free and extensible bone image analysis in ImageJ. *Bone* **47**, 1076-1079.

**Eming, S. A., Martin, P. and Tomic-Canic, M.** (2014). Wound repair and regeneration: mechanisms, signaling, and translation. *Sci Transl Med* **6**, 265sr266.

**Fernando, W. A., Leininger, E., Simkin, J., Li, N., Malcom, C. A., Sathyamoorthi, S., Han, M. and Muneoka, K.** (2011). Wound healing and blastema formation in regenerating digit tips of adult mice. *Dev Biol* **350**, 301-310.

**Frith, J. C., Mönkkönen, J., Blackburn, G. M., Russell, R. G. G. and Rogers, M. J.** (1997). Clodronate and Liposome-Encapsulated Clodronate Are Metabolized to a Toxic ATP Analog, Adenosine 5′-(β,γ-Dichloromethylene) Triphosphate, by Mammalian Cells In Vitro. *Journal of Bone and Mineral Research* **12**, 1358-1367.

**Gemberling, M., Bailey, T. J., Hyde, D. R. and Poss, K. D.** (2013). The zebrafish as a model for complex tissue regeneration. *Trends Genet* **29**, 611-620.
**Godwin, J. W., Pinto, A. R. and Rosenthal, N. A.** (2013). Macrophages are required for adult salamander limb regeneration. *Proc Natl Acad Sci U S A* **110**, 9415-9420.
**Godwin, J. W., Pinto, A. R. and Rosenthal, N. A.** (2016). Chasing the recipe for a pro-regenerative immune system. In *Seminars in cell & developmental biology*: Elsevier.
**Goren, I., Allmann, N., Yogev, N., Schürmann, C., Linke, A., Holdener, M., Waisman, A., Pfeilschifter, J. and Frank, S.** (2009). A transgenic mouse model of inducible macrophage depletion: effects of diphtheria toxin-driven lysozyme M-specific cell lineage ablation on wound inflammatory, angiogenic, and contractive processes. *The American journal of pathology* **175**, 132-147.
**Goss, R. J.** (1956). Regenerative inhibition following limb amputation and immediate insertion into the body cavity. *The Anatomical Record* **126**, 15-27.
**Grillo, H. C., Lapie, C. M., Dresden, M. H. and Gross, J.** (1968). Collagenolytic activity in regenerating forelimbs of the adult newt (Triturus viridescens). *Developmental biology* **17**, 571-583.
**Han, M., Yang, X., Lee, J., Allan, C. H. and Muneoka, K.** (2008). Development and regeneration of the neonatal digit tip in mice. *Dev Biol* **315**, 125-135.
**Hirsch, S. and Gordon, S.** (1983). Polymorphic expression of a neutrophil differentiation antigen revealed by monoclonal antibody 7/4. *Immunogenetics* **18**, 229-239.
**Illingworth, C. M.** (1974). Trapped fingers and amputated finger tips in children. *J Pediatr Surg* **9**, 853-858.
**Khan, U. A., Hashimi, S. M., Bakr, M. M., Forwood, M. R. and Morrison, N. A.** (2016). CCL2 and CCR2 are Essential for the Formation of Osteoclasts and Foreign Body Giant Cells. *Journal of cellular biochemistry* **117**, 382-389.
**Kyriakides, T. R., Foster, M. J., Keeney, G. E., Tsai, A., Giachelli, C. M., Clark-Lewis, I., Rollins, B. J. and Bornstein, P.** (2004). The CC chemokine ligand, CCL2/MCP1, participates in macrophage fusion and foreign body giant cell formation. *Am J Pathol* **165**, 2157-2166.
**Lehoczky, J. A. and Tabin, C. J.** (2015). Lgr6 marks nail stem cells and is required for digit tip regeneration. *Proc Natl Acad Sci U S A* **112**, 13249-13254.
**Leibovich, S. J. and Ross, R.** (1975). The role of the macrophage in wound repair. A study with hydrocortisone and antimacrophage serum. *Am J Pathol* **78**, 71-100.
**Li, S., Li, B., Jiang, H., Wang, Y., Qu, M., Duan, H., Zhou, Q. and Shi, W.** (2013). Macrophage depletion impairs corneal wound healing after autologous transplantation in mice. *PLoS One* **8**, e61799.
**Lucas, T., Waisman, A., Ranjan, R., Roes, J., Krieg, T., Muller, W., Roers, A. and Eming, S. A.** (2010). Differential roles of macrophages in diverse phases of skin repair. *J Immunol* **184**, 3964-3977.
**Mak, K., Manji, A., Gallant-Behm, C., Wiebe, C., Hart, D. A., Larjava, H. and Hakkinen, L.** (2009). Scarless healing of oral mucosa is characterized by faster resolution of inflammation and control of myofibroblast action compared to skin wounds in the red Duroc pig model. *J Dermatol Sci* **56**, 168-180.
**Martin, P., D'Souza, D., Martin, J., Grose, R., Cooper, L., Maki, R. and McKercher, S. R.** (2003). Wound healing in the PU.1 null mouse--tissue repair is not dependent on inflammatory cells. *Curr Biol* **13**, 1122-1128.
**Martin, P. and Leibovich, S. J.** (2005). Inflammatory cells during wound repair: the good, the bad and the ugly. *Trends Cell Biol* **15**, 599-607.
**McKim, L. H.** (1932). Regeneration of the Distal Phalanx. *Can Med Assoc J* **26**, 549-550.
**Mescher, A. L.** (1976). Effects on adult newt limb regeneration of partial and complete skin flaps over the amputation surface. *Journal of Experimental Zoology* **195**, 117-127.
**Mirza, R., DiPietro, L. A. and Koh, T. J.** (2009). Selective and specific macrophage ablation is detrimental to wound healing in mice. *Am J Pathol* **175**, 2454-2462.

**Mori, R., Kondo, T., Ohshima, T., Ishida, Y. and Mukaida, N.** (2002). Accelerated wound healing in tumor necrosis factor receptor p55-deficient mice with reduced leukocyte infiltration. *FASEB J* **16**, 963-974.

**Mori, R., Shaw, T. J. and Martin, P.** (2008). Molecular mechanisms linking wound inflammation and fibrosis: knockdown of osteopontin leads to rapid repair and reduced scarring. *J Exp Med* **205**, 43-51.

**Neufeld, D. A. and Zhao, W.** (1993). Phalangeal regrowth in rodents: postamputational bone regrowth depends upon the level of amputation. *Progress in clinical and biological research* **383a**, 243-252.

**Novak, M. L., Weinheimer-Haus, E. M. and Koh, T. J.** (2014). Macrophage activation and skeletal muscle healing following traumatic injury. *J Pathol* **232**, 344-355.

**Petrie, T. A., Strand, N. S., Yang, C. T., Rabinowitz, J. S. and Moon, R. T.** (2014). Macrophages modulate adult zebrafish tail fin regeneration. *Development* **141**, 2581-2591.

**Pfefferli, C. and Jazwinska, A.** (2015). The art of fin regeneration in zebrafish. *Regeneration (Oxford, England)* **2**, 72-83.

**Raggatt, L. J., Wullschleger, M. E., Alexander, K. A., Wu, A. C., Millard, S. M., Kaur, S., Maugham, M. L., Gregory, L. S., Steck, R. and Pettit, A. R.** (2014). Fracture healing via periosteal callus formation requires macrophages for both initiation and progression of early endochondral ossification. *Am J Pathol* **184**, 3192-3204.

**Russell, R. G. and Rogers, M. J.** (1999). Bisphosphonates: from the laboratory to the clinic and back again. *Bone* **25**, 97-106.

**Sammarco, M. C., Simkin, J., Cammack, A. J., Fassler, D., Gossmann, A., Marrero, L., Lacey, M., Van Meter, K. and Muneoka, K.** (2015). Hyperbaric Oxygen Promotes Proximal Bone Regeneration and Organized Collagen Composition during Digit Regeneration. *PLoS One* **10**, e0140156.

**Sammarco, M. C., Simkin, J., Fassler, D., Cammack, A. J., Wilson, A., Van Meter, K. and Muneoka, K.** (2014). Endogenous bone regeneration is dependent upon a dynamic oxygen event. *J Bone Miner Res* **29**, 2336-2345.

**Schindeler, A., McDonald, M. M., Bokko, P. and Little, D. G.** (2008). Bone remodeling during fracture repair: The cellular picture. *Seminars in cell & developmental biology* **19**, 459-466.

**Simkin, J., Han, M., Yu, L., Yan, M. and Muneoka, K.** (2013). The mouse digit tip: from wound healing to regeneration. *Methods Mol Biol* **1037**, 419-435.

**Simkin, J., Sammarco, M. C., Dawson, L. A., Tucker, C., Taylor, L. J., Van Meter, K. and Muneoka, K.** (2015a). Epidermal closure regulates histolysis during mammalian (Mus) digit regeneration. *Regeneration* **2**, 14.

**Simkin, J., Sammarco, M. C., Dawson, L. A., Tucker, C., Taylor, L. J., Van Meter, K. and Muneoka, K.** (2015b). Epidermal closure regulates histolysis during mammalian (Mus) digit regeneration. *Regeneration (Oxford, England)* **2**, 106-119.

**Sinder, B. P., Pettit, A. R. and McCauley, L. K.** (2015). Macrophages: Their Emerging Roles in Bone. *J Bone Miner Res* **30**, 2140-2149.

**Sprangers, S., de Vries, T. J. and Everts, V.** (2016). Monocyte Heterogeneity: Consequences for Monocyte-Derived Immune Cells. *J Immunol Res* **2016**, 1475435.

**Stocum, D. L.** (2012). *Regenerative biology and medicine*: Academic Press.

**Stocum, D. L. and Cameron, J. A.** (2011). Looking proximally and distally: 100 years of limb regeneration and beyond. *Dev Dyn* **240**, 943-968.

**Takeo, M., Chou, W. C., Sun, Q., Lee, W., Rabbani, P., Loomis, C., Taketo, M. M. and Ito, M.** (2013). Wnt activation in nail epithelium couples nail growth to digit regeneration. *Nature* **499**, 228-232.

**Tanaka, E. M.** (2003). Regeneration: if they can do it, why can't we? *Cell* **113**, 559-562.

**van Rooijen, N. and Hendrikx, E.** (2010). Liposomes for specific depletion of macrophages from organs and tissues. *Methods Mol Biol* **605**, 189-203.

**Vinarsky, V., Atkinson, D. L., Stevenson, T. J., Keating, M. T. and Odelberg, S. J.** (2005). Normal newt limb regeneration requires matrix metalloproteinase function. *Dev Biol* **279**, 86-98.

**Whitehead, G. G., Makino, S., Lien, C.-L. and Keating, M. T.** (2005). fgf20 Is Essential for Initiating Zebrafish Fin Regeneration. *Science* **310**, 1957-1960.

**Winkler, I. G., Sims, N. A., Pettit, A. R., Barbier, V., Nowlan, B., Helwani, F., Poulton, I. J., van Rooijen, N., Alexander, K. A., Raggatt, L. J., et al.** (2010). Bone marrow macrophages maintain hematopoietic stem cell (HSC) niches and their depletion mobilizes HSCs. *Blood* **116**, 4815-4828.

**Xiang, S., Dong, H. H., Liang, H. F., He, S. Q., Zhang, W., Li, C. H., Zhang, B. X., Zhang, B. H., Jing, K., Tomlinson, S., et al.** (2012). Oval cell response is attenuated by depletion of liver resident macrophages in the 2-AAF/partial hepatectomy rat. *PLoS One* **7**, e35180.

**Xue, M. and Jackson, C. J.** (2015). Extracellular Matrix Reorganization During Wound Healing and Its Impact on Abnormal Scarring. *Advances in wound care* **4**, 119-136.

**Yang, E. V. and Bryant, S. V.** (1994). Developmental regulation of a matrix metalloproteinase during regeneration of axolotl appendages. *Dev Biol* **166**, 696-703.

**Yang, E. V., Gardiner, D. M., Carlson, M. R., Nugas, C. A. and Bryant, S. V.** (1999). Expression of Mmp-9 and related matrix metalloproteinase genes during axolotl limb regeneration. *Dev Dyn* **216**, 2-9.

**Zeisberger, S. M., Odermatt, B., Marty, C., Zehnder-Fjallman, A. H., Ballmer-Hofer, K. and Schwendener, R. A.** (2006). Clodronate-liposome-mediated depletion of tumour-associated macrophages: a new and highly effective antiangiogenic therapy approach. *Br J Cancer* **95**, 272-281.

## Figures

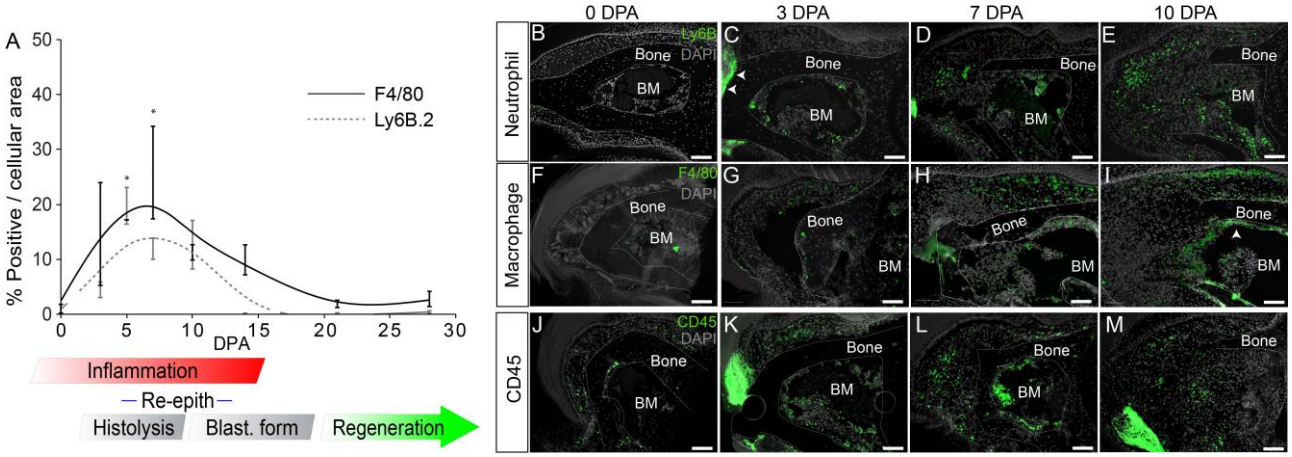


**Figure 1. Leukocytes are recruited to the injury site after amputation.** (A) Macrophage and neutrophils numbers are quantified using immunohistochemistry for the pan-macrophage marker, F4/80, and the neutrophil cell surface protein, Ly6B.2. Both macrophage and neutrophil numbers increase at the wound site temporarily following a regenerative P3 amputation. Stages of regeneration are delineated beneath the graph: Inflammation, Histolysis, Re-epithelization, Blastema formation, and Regeneration. (*Bonferrori post hoc test $p<0.05$ for Ly6B.2 0 DPA vs. 5 DPA and F4/80 0 DPA vs. 7 DPA. n=3/timepoint). **(B-E)** Ly6B.2 + cells (green) are observed in the injury area after amputation, in low numbers at 0 DPA (B), in the bone marrow and in scab (white arrows) at 3 DPA (C), and in the forming blastema and bone marrow at 7 DPA (D) and 10 DPA (E). **(F-I)** F4/80+ macrophages (green) are observed in low numbers at 0 DPA (F) and 3 DPA (G). At 7 DPA F4/80+ macrophages localize to the soft connective tissue surrounding the bone stump and in the bone marrow (H). By 10 DPA the blastema is formed and F4/80+ macrophages are present in the connective tissue surrounding the bone stump and lining the endosteal layer (white arrowhead) of the bone marrow cavity (I). F4/80+ macrophages are notably absent from the blastema proper. **(J-M)** Presence of CD45 + leukocytes (green) surrounding the P3 digit is low at 0 DPA (J) and increases after amputation at 3 DPA (K), 7 DPA (L) and 10 DPA (M). Grey = DAPI nuclear stain, Scale bars = 100µm. DPA = days post amputation. BM = Bone marrow. For all images: distal = left, dorsal = top

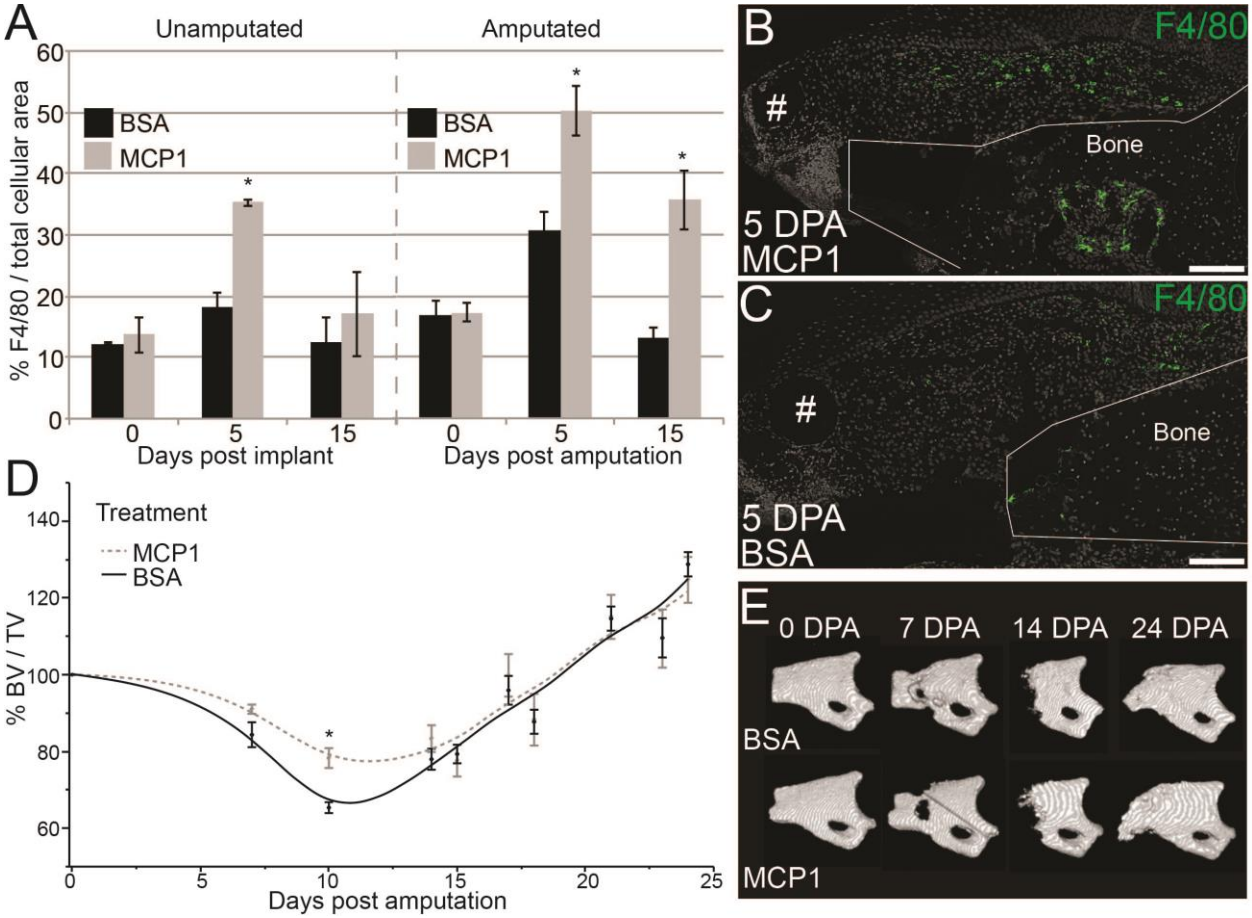


**Figure 2. Increasing macrophage numbers does not inhibit regenerative ability. (A)** The introduction of monocyte chemoattractant protein-1 (MCP1) via a microcarrier bead is able to recruit a higher number of F4/80+ cells to P3 when compared to BSA control beads both in unamputated digits and following amputation. Y-axis = total area of F4/80 + signal per total area of DAPI + signal in the connective tissue area. X-axis = days post bead implantation in unamputated and amputated digits (n=7 mice, 14 digits per treatment, *Bonferrori post hoc test $p<0.05$ for main effect treatment) **(B-C)** Immunofluorescence with anti F4/80 at 5 DPA after implantation of microcarrier beads soaked in MCP1 (B) or BSA (C). Green= F4/80, Grey = DAPI, # = microcarrier bead. Scale bars = 100μm **(D)** Micro-CT analysis of bone volume change over time. MCP1 treated digits show a significant reduction in amount of bone degradation when compared to BSA controls, but show the same overall bone volume growth by DPA 24 as compared to BSA controls. Y-axis = percent bone volume per total volume at time of amputation (%BV/TV). X-axis = Days post amputation. (n=7 mice, 14 digits per treatment, *Bonferroni post hoc test $p<0.05$ for main effect treatment). **(E)** 3D renderings of μCT data show patterned bone growth in both BSA and MCP1 treated digits by 24 DPA. For all images: distal = left, dorsal = top

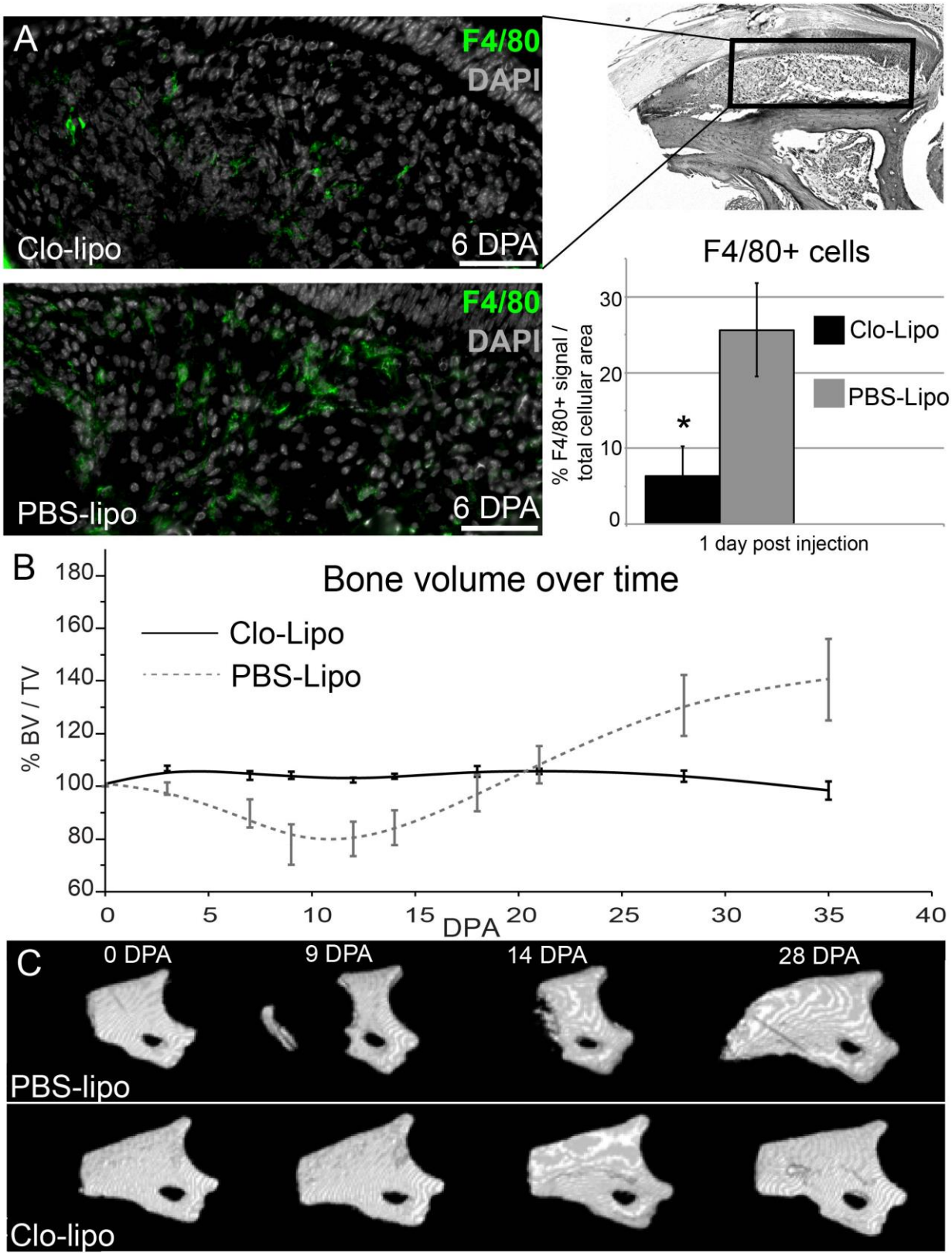


**Figure 3. Local injections of clodronate liposomes effectively deplete macrophage populations and inhibit regeneration. (A)** 50μg of either clodronate liposomes (Clo-Lipo) or PBS liposomes (PBS-Lipo) were locally injected into the P2 digit at days 0, 2, and 5 after amputation. Quantification of F4/80+ cells at 6 days post amputation (1 day post final injection) reveal a significant reduction in the number of activated macrophages in P3. Green = F4/80; Grey = DAPI. Scale bar = 50μm Y-axis

= % F4/80+ signal per total DAPI + signal in connective tissue area (*unpaired Student's t-test $p<0.05$). **(B)** μCT analysis of bone volume changes over time show PBS-lipo treated animals have a normal regeneration response which includes first a loss of bone volume followed by bone regeneration (n=4 mice, 16 digits). In contrast, Clo-Lipo treated animals exhibit a complete inhibition of both bone degradation and bone regrowth over the course of 35 days post amputation (n=4 mice, 16 digits) **(C)** 3D renderings of μCT scans enable visualization of the bone loss and regeneration in PBS-lipo treated animals. In Clo-lipo treated animals, there are no significant changes to bone architecture. For all images: distal = left, dorsal = top

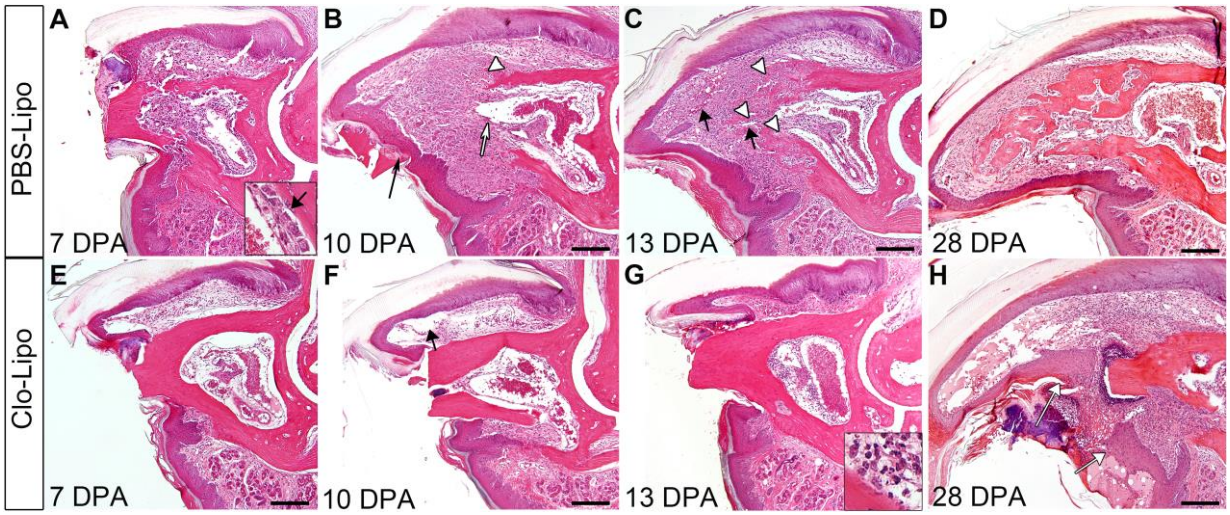


**Figure 4. Injections of clodronate liposomes inhibit histolysis and epidermal closure. (A-D)** H&E staining of P3 digits over the course of regeneration in PBS-Lipo treated digits. By 7 DPA (A), digits display bone degradation and endosteal activation (inset arrow). By 10 DPA (B) digits have a closed epidermis which ejects degraded bone fragments (black arrow), blastema formation contiguous with the bone marrow (white arrow) and the beginnings of new bone formation (white arrow head). By 13 DPA (C), new blood vessels have formed (black arrows) distal to the newly regenerating bone (white arrowheads). By 28 DPA (D), bone continues to be remodeled in trabecular islands. **(E-H)** H&E staining of P3 digits following Clo-Lipo injections show an open epidermis and lack of bone degradation at 7 DPA (E). Distal nail and epidermal growth (black arrow) is evident at 10 DPA (F) but not epidermal closure. At 13 DPA, there is a lack of re-epithelization, no bone degradation is observed and there is no blastema formation evident. Cell accumulation in the marrow consists of polymorphonuclear cells (inset). The epidermis has failed to close by 28 DPA (H white arrows) though distal epidermal and nail growth is evident. Scale bar = 200μm. For all images: distal = left, dorsal = top

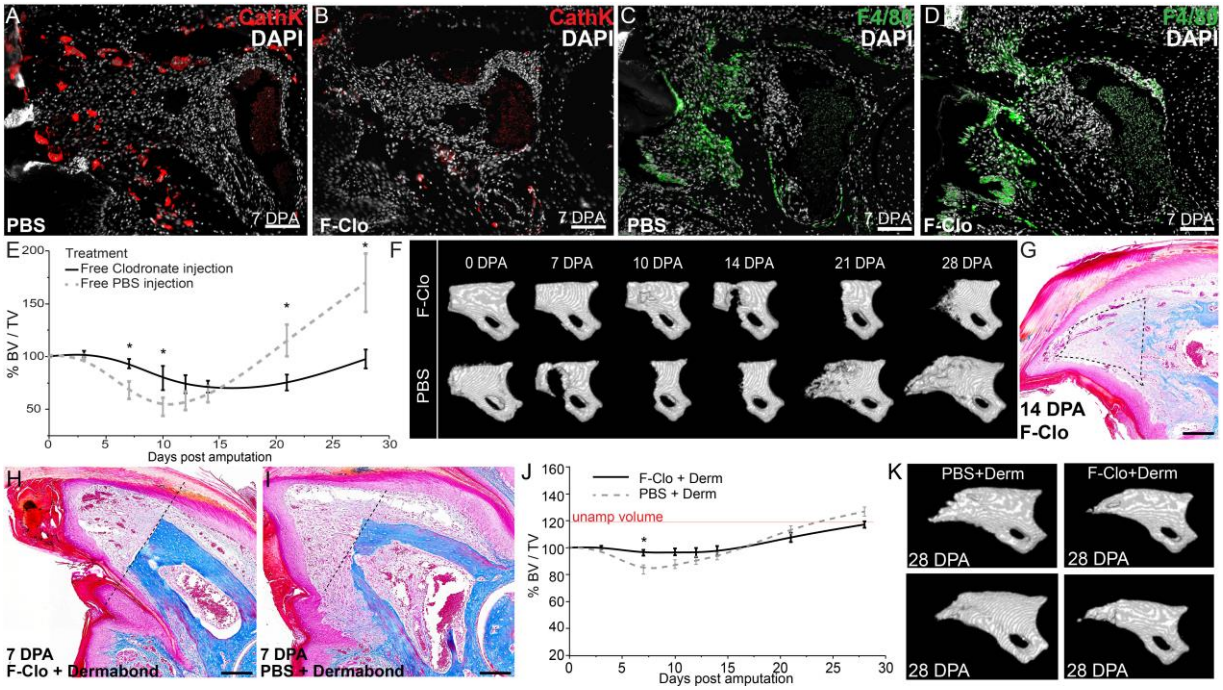


**Figure 5. Osteoclast-specific depletion delays but does not inhibit regeneration. (A-B)** A single injection of free clodronate (F-Clo) immediately following amputation depletes the P3 digit of Cathepsin K+ (CathK, red) cells. Representative image of a PBS-injected control digit (A) and a F-Clo injected digit (B) at 7 days post amputation (DPA). Scale bar = 100μm **(C-D)** F4/80+ staining (green) in PBS-injected digit (C) and F-Clo injected digit (D) at 7 DPA showing macrophage localization to cells surrounding the bone stump. Scale bar = 100μm. Grey = DAPI nuclear stain. **(E)** μCT analysis of bone volume changes with time after amputation in PBS treated digits (grey dotted line) and F-Clo treated digits (black line). Changes are measured in percent bone volume/total volume at time of amputation (%BV/TV). n=4 mice, 16 digits for both groups, *Bonferroni post hoc test $p<0.05$ main effect treatment at time points indicated. **(F)** 3D renderings of μCT images for PBS treated and F-Clo treated digits over time. **(G)** Trichrome staining of F-Clo treated digit at 14 DPA showing complete re-epithelization and accumulation of cells in the distal mesenchyme (dotted outline). Scale bar = 100μm. **(H-I)** Digits were treated with either F-Clo and Dermabond (H) or PBS and Dermabond (I). Trichrome staining reveals a loss of bone degradation from the original plane of amputation (black dotted line) in F-Clo+Derm treated digits and only minor degradation in PBS+Derm treated digits. Scale bar = 100μm **(J)** Micro-CT to track bone volume changes measured in percent bone volume/total volume at time of amputation (%BV/TV). Digits were treated with combined F-Clo and Dermabond (black line) or combined PBS and Dermabond (grey dotted line). In both treatment groups, bone regenerates to pre-amputation levels (red line). n=4 mice, 16 digits for both groups. *Bonferroni post hoc test $p<0.05$ main effect treatment. **(K)** Representative μCT images of P3 bone in either combined PBS and Dermabond treatment or combine F-Clo and Dermabond treatment groups at 28 DPA showing patterned bone growth in both groups. For all images: distal = left, dorsal = top

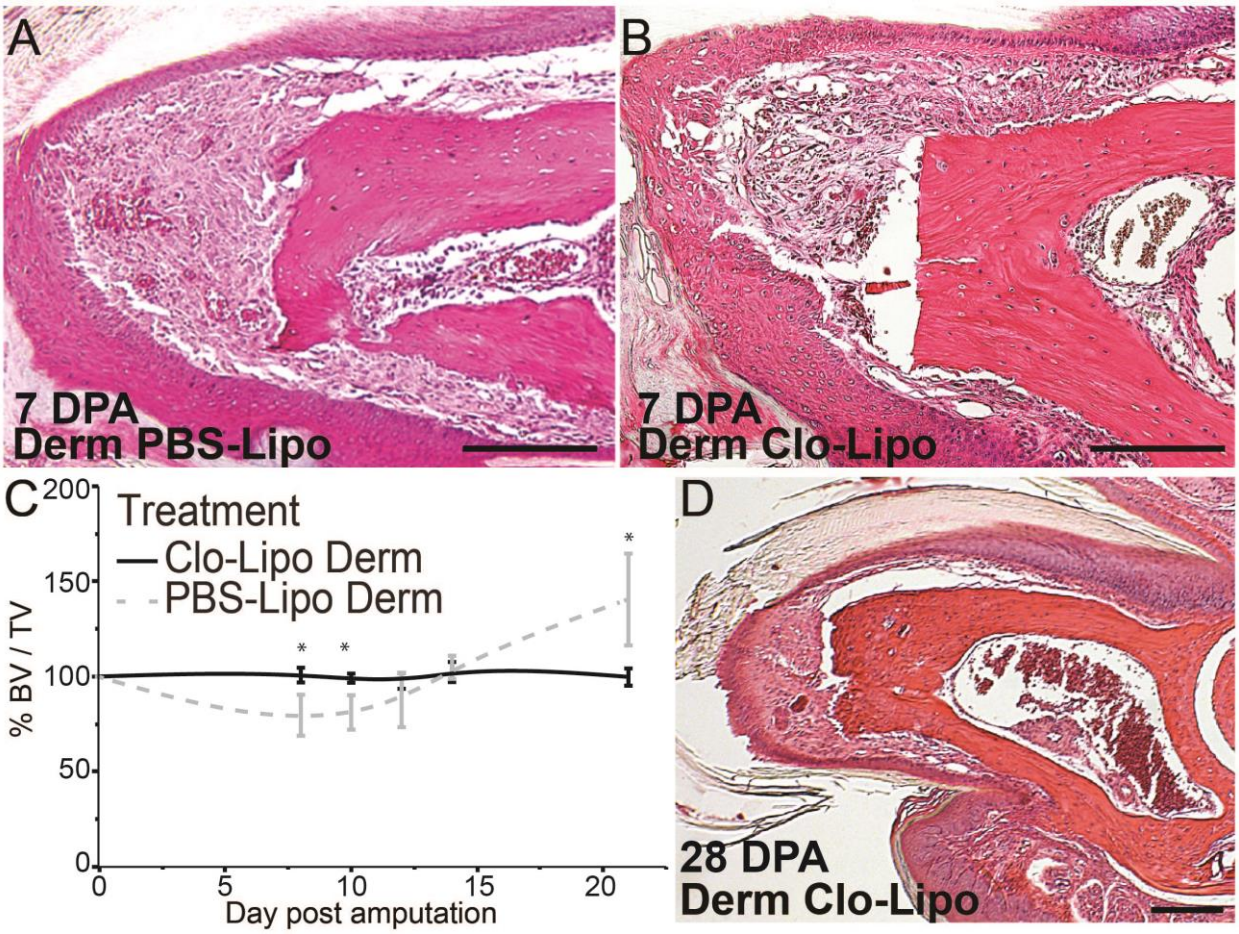


**Figure 6. Rescuing epidermal closure does not rescue regeneration in Clo-Lipo treated digits.** **(A-B)** H&E staining for histology shows application of Dermabond promotes epidermal closure and accumulation of mesenchymal cells under the epidermis by 7 DPA in PBS-Lipo treated digits (A) and Clo-Lipo treated digits (B). Scale bars = 100μm. **(C)** Micro-CT analysis of bone volume change over time reveals a loss of regeneration response in Clo-Lipo treated digits despite the rescue of epidermal closure. Y-axis = percent bone volume over total volume at time of amputation (%BV/TV), X-axis = days post amputation, n=8 digits for Clo-Lipo+Derm, n=4 digits for PBS-Lipo+Derm, (*Bonferroni post hoc test $p<0.05$, main effect treatment at timepoints indicated). **(D)** H&E of Dermbond treated, Clo-Lipo injected digits at 28 DPA shows no evidence of bone degradation or regrowth. Scale bar = 100μm. For all images: distal = left, dorsal = top

## SUPPLEMENTAL FIGURES

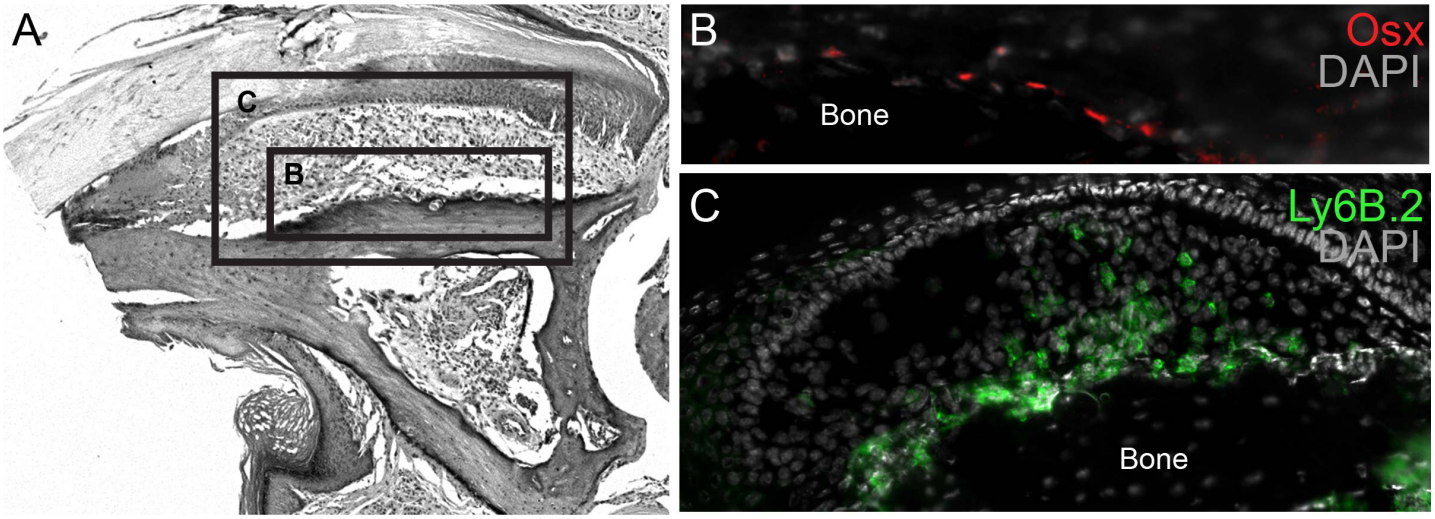


**Supplemental Figure 1. Clo-Lipo injections do not deplete osteoblast or neutrophil populations. (A)** Map of amputated digit at 5 DPA showing area represented in images (B) and (C). **(B)** 1 day post Clo-Lipo injection, Osx+ cells are still present and line the periosteum of the amputated bone, however the Osx+ cells maintain a squamous morphology associated with quiescent osteoblasts. **(C)** Immunohistochemical stain for the neutrophil cell surface marker Ly6B.2. Neutrophils are still present at the injury site 1 day after the final Clo-Lipo injections (6 days post amputation).

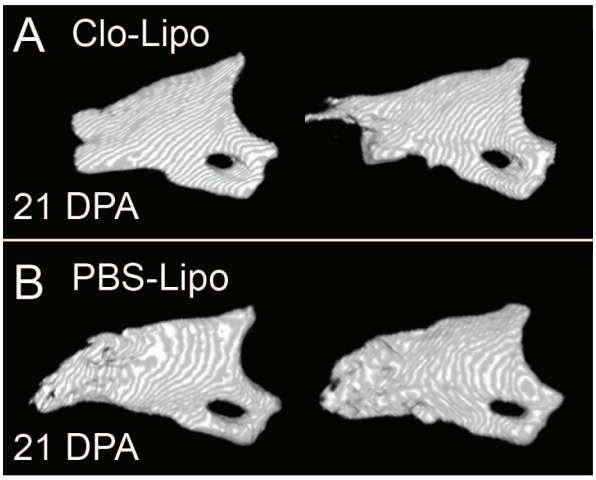


**Supplemental Figure 2. A single injection of Clo-Lipo or PBS-Lipo at 0 DPA immediately following amputation results in partial inhibition of regeneration. (A)** 3D renderings of μCT scans of Clo-Lipo treated digits at 21 days post amputation (DPA). 3 out of 8 digits treated with Clo-Lipo at 0 DPA show no degradation or new bone growth by 21 DPA whereas 5/8 digits show unpatterned bone growth. **(B)** Digits treated with PBS-Lipo at 0 DPA show patterned bone growth by 21 DPA.

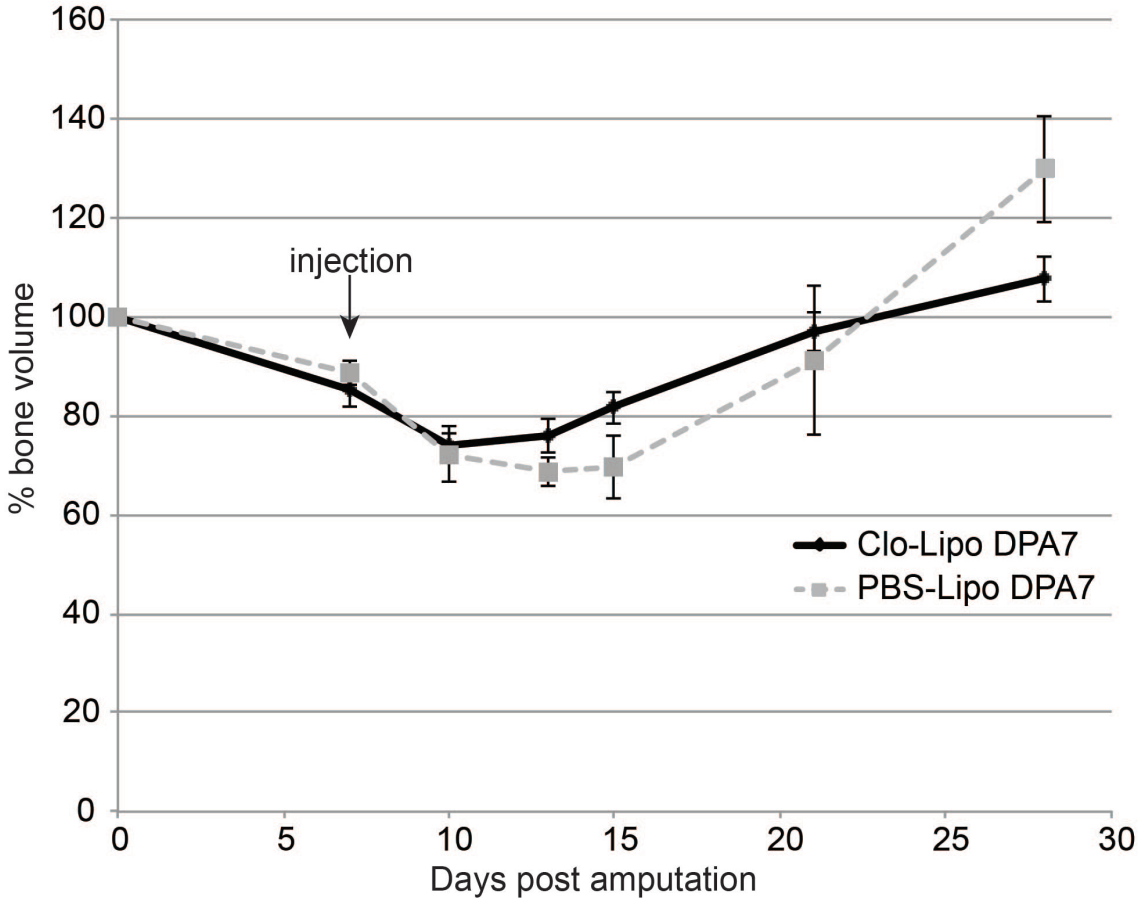


**Supplemental Figure 3**. A single injection of Clo-Lipo at 7 DPA does not inhibit regeneration. Clo-Lipo or PBS-Lipo was injected at 7 DPA (arrow) when macrophages and osteoclasts are at peak activity. Clo-Lipo treated digits (black line) show a trend toward less bone growth compared to PBS-Lipo treated digits (grey dotted line) but differences in final volumes are not statistically significant (Two-way ANOVA main effect time, $F=25.72$, $p<0.0001$, and main effect treatment $F=0.002$, $p=0.97$). Y-axis = %bone volume / total volume at time of amputation. X-axis = Days post amputation